

See discussions, stats, and author profiles for this publication at:  
<https://www.researchgate.net/publication/244352292>

# The effect of ligand donor atoms on the regioselectivity in the palladium catalyzed allylic alkylation

ARTICLE in *INORGANICA CHIMICA ACTA* · JANUARY 2002

Impact Factor: 2.05 · DOI: 10.1016/S0020-1693(01)00694-6

CITATIONS

21

READS

24

9 AUTHORS, INCLUDING:



**Kees Goubitz**

Delft University of Technology

244 PUBLICATIONS 4,318 CITATIONS

SEE PROFILE



**Joost N H Reek**

University of Amsterdam

386 PUBLICATIONS 10,826 CITATIONS

SEE PROFILE



**Paul C J Kamer**

University of St Andrews

276 PUBLICATIONS 10,121 CITATIONS

SEE PROFILE



**Piet W N M van Leeuwen**

Institut National des Sciences Appliquées...

505 PUBLICATIONS 17,543 CITATIONS

SEE PROFILE



# The effect of ligand donor atoms on the regioselectivity in the palladium catalyzed allylic alkylation

Richard J. van Haaren <sup>a</sup>, Peter H. Keeven <sup>a</sup>, Lars A. van der Veen <sup>a</sup>, Kees Goubitz <sup>a</sup>,  
Gino P.F. van Strijdonck <sup>a</sup>, Henk Oevering <sup>b</sup>, Joost N.H. Reek <sup>a</sup>, Paul C.J. Kamer <sup>a</sup>,  
Piet W.N.M. van Leeuwen <sup>a,\*</sup>

<sup>a</sup> Institute of Molecular Chemistry, University of Amsterdam, Nieuwe Achtergracht 166, 1018 WV Amsterdam, The Netherlands

<sup>b</sup> DSM Research BV, Postbus 18, 6160 MD Geleen, The Netherlands

Received 11 May 2001; accepted 27 August 2001

Dedicated to Professor Dr Kees Vrieze for his outstanding contributions to coordination and organometallic chemistry in general and palladium allyl chemistry in particular

## Abstract

The regioselectivity of the palladium catalyzed allylic alkylation was studied systematically using bidentate ligands based on a xanthene backbone, bearing different donor atoms. The nature of the ligand donor atoms has a pronounced influence on the regioselectivity of the reaction. The results can be explained by a mechanism that distinguishes two ‘stages’ in the alkylation reaction. Ligands bearing strong  $\pi$ -acceptor donor atoms induce the formation of branched products (60% for the P–P derivative), whereas the use of ligands with weak  $\pi$ -acceptor donor atoms mainly yields linear products (>99% for the N–N derivative).  
© 2002 Elsevier Science B.V. All rights reserved.

**Keywords:** Crystal structures; Palladium complexes; Bidentate ligand complexes; Allylic alkylation

## 1. Introduction

The palladium catalyzed allylic alkylation is a useful tool in synthetic organic chemistry [1]. Much research has been devoted to optimizing and understanding the enantioselectivity of the reaction, mainly using substrates such as *Z*-cyclohex-2-enyl acetate, *E*-1,3-diphenyl-prop-2-enyl-1 acetate or related compounds [1–3]. In the catalytic cycle, these substrates add oxidatively to Pd(0) to form (ligand)Pd<sup>II</sup>( $\pi$ -allyl)OAc complexes, bearing a symmetrically substituted allyl group. Carbon–carbon bond formation by nucleophilic attack takes place at one of the two terminal allylic carbon atoms and consequently a chiral product is formed (Fig. 1). The structure of palladium allyl complexes has

been studied in detail and in the late 1960s and early 1970s Vrieze showed by elegant NMR studies that these complexes are very dynamic [4]. This dynamic behavior can have a large impact on the selectivity of the reaction, particularly when non-symmetric substrates are used.

When substrates that form a non-symmetric  $\pi$ -allyl complex are used, regiocontrol becomes an issue in addition to enantiocontrol (Fig. 2) [5–8].

Compared with the vast amount of studies towards the enantioselective allylic alkylation, relatively few studies are concerned with the regioselectivity of this reaction [5–17].

Previously, we reported on the effect of the (P–Pd–P) bite angle of bidentate phosphine ligands on the regioselectivity [10,16]. It was found that for the allylic alkylation of *E*-hex-2-enyl acetate (R = propyl, R' = H), attack at the non-substituted (R' = H), is favored for all the ligands examined, leading to the non-chiral linear product. The use of ligands enforcing a larger

\* Corresponding author. Tel.: +31-20-525 5419; fax: +31-20-525 6456.

E-mail address: pwnm@anorg.chem.uva.nl (P.W.N.M. van Leeuwen).

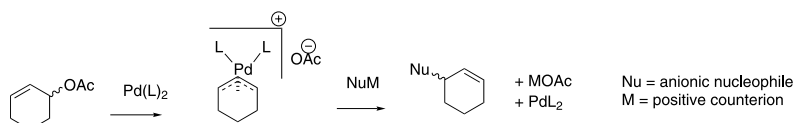
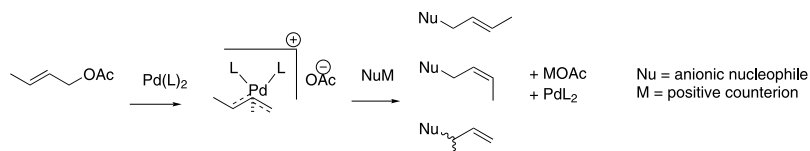


Fig. 1. Allylic alkylation of cyclohexenyl acetate.

Fig. 2. Allylic alkylation of a non-symmetric  $\pi$ -allyl complex.

bite angle leads to an increase of the regioselectivity to the linear product up to 100%. These results were explained in terms of steric hindrance: a larger bite angle of the ligand results in a larger cone angle of the ligand.

Recently, several authors have reported on a relation between the symmetry of the palladium- $\pi$ -allyl bond and the regioselectivity [11,15,17]. A distortion of the symmetry of the Pd-allyl bond leads to activation for the nucleophilic attack of the allylic carbon atom having the largest Pd-C distance. For bidentate PP ligands, we showed that in the crystal structures of a series of (P-P)Pd(1,1-(CH<sub>3</sub>)<sub>2</sub>-C<sub>3</sub>H<sub>3</sub>)OTf complexes the symmetry of the Pd-allyl bond depends on the cone angle of the P-P ligand (Fig. 3) [17]. As a result of the increased steric hindrance, a large cone angle of the ligand results in a large distortion of the Pd- $\eta^3$ -C<sub>3</sub>H<sub>5</sub> bond. The bond is almost symmetric in the dppe (1,2-(bis(diphenylphosphino)ethane) modified complex while in the DPEphos (bis(2-diphenylphosphino-phenyl)-ether, Fig. 3) modified complex the Pd-allyl bond is significantly distorted to an  $\eta^1$ - $\eta^2$  bonding mode (Fig. 4). Due to this distortion, the 1,1-dimethyl substituted carbon atom (C3) is more electrophilic than the non-substituted allylic carbon atom (C1). A larger distortion resulted in a larger difference in electrophilicity between the terminal carbon atoms. Stoichiometric reaction of these complexes with a nucleophile (sodium diethyl 2-methyl-malonate) led to the formation of two regioisomeric products. Attack on the unsubstituted carbon atom (C1) yields the linear olefin **B** and attack on the substituted carbon atom (C3) yields the branched olefin **A**. The regioselectivity of the reaction varied from 8/92 (**B/A**) for dppe to 60/40 for Xantphos [17]. Thus, the trend in the regioselectivity observed for the 3-methyl-butenyl complexes is opposite to that found for the alkylation of *E*-hex-2-enyl acetate [10].

Among others, Vrieze and coworkers [18] showed that the nature of the donor atoms is an important factor in the allylic alkylation. To gain more insight into the factors determining the regioselectivity of the

reaction, we decided to explore the *electronic* effect of ligands that all enforce a large bite angle, but differ in the nature of the donor atoms (Fig. 5) [19]. Using these ligands, we prepared a series of cationic (3-methyl-butenyl)Pd(ligand) complexes and used them in the stoichiometric allylic alkylation.

## 2. Experimental

### 2.1. General procedures

<sup>1</sup>H NMR (300 MHz, TMS, CDCl<sub>3</sub>), <sup>31</sup>P{<sup>1</sup>H} (121.5 MHz external 85% H<sub>3</sub>PO<sub>4</sub>, CDCl<sub>3</sub>) were recorded in a Bruker AMX-300 spectrometer. The product distribution of allylic alkylation was measured by GC in an Interscience Mega2 apparatus, equipped with a DB1 column, length 30 m, inner diameter 0.32 mm, film thickness 3.0  $\mu$ m, and a F.I.D detector. All experiments were carried out using standard Schlenk techniques. All solvents were freshly distilled prior to use. All reactions have been performed at room temperature (r.t.) (292 K). Sodium diethyl 2-methylmalonate (0.5 M in THF) was prepared from diethyl 2-methylmalonate and NaH in THF at 273 K.

### 2.2. Ligand syntheses

The syntheses of ligands **a–e** have been published elsewhere [19].

#### 2.2.1. Synthesis of ligand **f**

One gram (4.8 mmol) of xanthene was dissolved in 50 ml of diethyl ether and 2.2 ml (14.3 mmol) of TMEDA

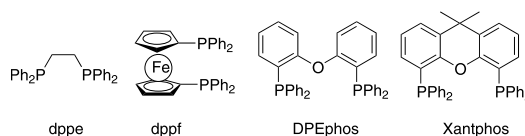


Fig. 3. Diphosphine ligands used in Ref. [13].

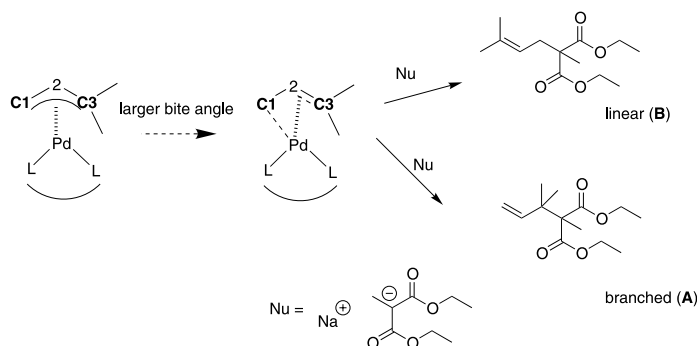


Fig. 4. Distortion of the Pd–allyl bond in (allyl)Pd(PP) complexes and products of the allylic alkylation [17].

was added. After cooling to 273 K, 11 ml (1.3 M in cyclohexane, 14.3 mmol) of *sec*-BuLi was added slowly to the solution. The reaction mixture was stirred for 20 h at 293 K. After cooling to 203 K, 0.458 g (14.3 mmol) of  $S_8$  was added and the reaction mixture was warmed slowly to 293 K (6 h). After cooling to 195 K, 1.2 ml (19.0 mmol) of MeI was added and the reaction mixture was stirred overnight at r.t. After 20 h, water was added and the mixture was extracted with  $CH_2Cl_2$  and water. The organic fractions were dried over  $Na_2SO_4$  and the crude product was further purified by column chromatography using 5% ethyl acetate in PE 60/80. Recrystallization from  $CH_2Cl_2$ –hexane yielded 0.42 g of **f** (29%) as white crystals.  $^1H$  NMR ( $CDCl_3$ ):  $\delta$  1.61 (s, 6H,  $CH_3$ ), 2.53 (s, 6H,  $SCH_3$ ), 7.09 (d, 4H, ArH,  $J = 4.7$  Hz), 7.22 (t, 2H, ArH,  $J = 4.7$  Hz).

### 2.3. Complex syntheses

The Pd-complexes were prepared in  $CH_2Cl_2$  from  $[(C_5H_9)_2Pd-\mu Cl]_2$  [20] by adding 2 equiv. of ligand and abstracting the chloride with AgOTf [17]. The complexes were isolated in quantitative yield (microcrystalline powder) and were used as such in the alkylation reaction. The synthesis and characterization of complex **1a** is described elsewhere [17].

#### 2.3.1. Characterization of **1b**

Major isomer (70%):  $^1H$  NMR:  $\delta$  1.10 (br b, 18H, t-Bu), 1.25 (br b, 6H,  $C(CH_3)_2$ ), 1.41 (br b, 3H, allyl  $CH_3$ -*anti*), 1.86 (br b, 3H, allyl  $CH_3$ -*syn*), 3.06 (br d, 1H,  $J = 13$  Hz, H-*anti*), 3.50 (br b, 1H, H-*syn*), 5.71 (br m, 1H, H-*meso*), 6.5–7.6 (m, 24H, H-aromatic).  $^{31}P$  NMR:  $\delta$  10.9.

Minor isomer (30%):  $^1H$  NMR:  $\delta$  1.10 (br b, 18H, t-Bu), 1.25 (br b, 6H,  $C(CH_3)_2$ ), 1.3 (br b, 3H, allyl  $CH_3$ -*anti*), 1.75 (br b, 3H, allyl  $CH_3$ -*syn*), 3.81 (br b, 1H, H-*anti*), 4.2 (br m, 1H, H-*syn*), 5.7 (br m, 1H, H-*meso*), 6.5–7.6 (m, 24H, H-aromatic).  $^{31}P$  NMR:  $\delta$  7.6.

HR MS;  $m/z$ : requires 910.2476 ( $C_{52}H_{58}AsOPPd^+$ ), found 909.2405 ( $C_{50}H_{58}AsOPPdNa^+$ ).

#### 2.3.2. Characterization of **1c**

$^1H$  NMR:  $\delta$  1.06 (br s, 9 H, t-Bu), 1.23 (br s, 9 H, t-Bu), 1.53 (br b, 6H,  $C(CH_3)_2$ ), 1.85 (br b, 6H, allyl  $CH_3$ -*syn* + *anti*), 2.15 (br b, 2H, allyl-H-*syn* + *anti*), 4.21 (br b, 1H, H-*meso*), 6.3–7.6 (m, 24H, H-aromatic).  $^{31}P$  NMR:  $\delta$  22.2 (br b).

HR MS;  $m/z$ : requires 849.3291 ( $C_{52}H_{58}NOPPd^+$ ), found 848.3190 ( $C_{50}H_{58}AsOPPdNa^+$ ).

#### 2.3.3. Characterization of **1d**

$^1H$  NMR:  $\delta$  1.11 (br s, 21 H, t-Bu + allyl  $CH_3$ -*anti*), 1.33 (br s, allyl- $CH_3$ -*syn*), 1.65 (br s, 6H,  $C(CH_3)_2$ ), 3.27 (d, 1H,  $J = 13$  Hz, H-*anti*), 3.81 (d, 1H,  $J = 6$  Hz, H-*syn*), 5.69 (dd, 1H,  $J_1 = 13$  Hz,  $J_2 = 6$  Hz, H-*meso*), 6.6–7.6 (m, 24H, H-aromatic).

HR MS;  $m/z$ : requires 953.1876 ( $C_{52}H_{58}As_2OPd^+$ ), found 953.1913.

#### 2.3.4. Characterization of **1e**

$^1H$  NMR:  $\delta$  1.26 (br s, 24H (t-Bu + ligand  $CH_3$ ), 1.70 (br s, 6H, allyl- $CH_3$ 's), 2.87 (d, 1H,  $J = 12$  Hz, H-*anti*), 3.85 (d, 1H,  $J = 7$  Hz, H-*syn*), 5.64 (dd, 1H,  $J_1 = 12$  Hz,  $J_2 = 7$  Hz, H-*meso*), 6.5–7.5 (br m, 24H).

#### 2.3.5. Characterization of **1f**

HR MS;  $m/z$ : requires 478.0616 ( $C_{22}H_{28}OPdS_2$ ), found 478.0624.

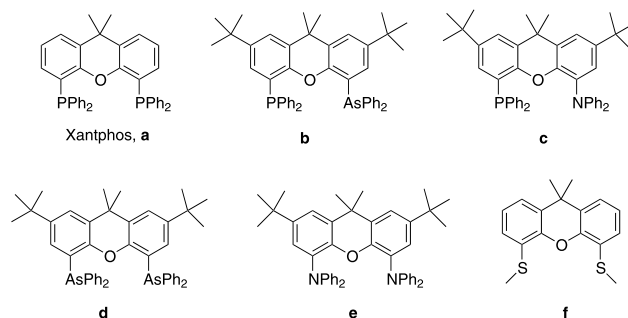


Fig. 5. Structure of xanthene-based ligands used in this work.

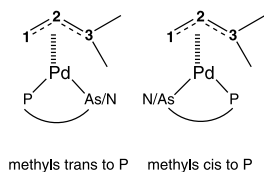


Fig. 6. Different isomeric structures of **1b** and **1c**.

#### 2.4. Allylic alkylation

The stoichiometric alkylation reactions were performed by adding an excess of sodium diethyl 2-methylmalonate (0.1 ml of a 0.5 M solution in THF) to a solution of 10 mg of the Pd-complex in 1 ml of THF. Reaction was instantaneous and after 1 min, the mixture was worked up with water, filtered over silica and analyzed by GC. All alkylation experiments were carried out in triplo.

#### 2.5. Structure determination

A crystal with dimensions approximately  $0.20 \times 0.30 \times 0.40$  mm was used for data collection in an Enraf–Nonius CAD-4 diffractometer with graphite-monochromated Cu K $\alpha$  radiation and  $\omega$ – $2\theta$  scan. A total of 5131 unique reflections was measured within the range  $-9 \leq h \leq 10$ ,  $0 \leq k \leq 15$ ,  $0 \leq l \leq 31$ . Of these, 4225 were above the significance level of  $4\sigma(F_{\text{obs}})$  and were treated as observed. The range of  $(\sin \theta)/\lambda$  was  $0.040$ – $0.626$  Å $^{-1}$  ( $3.5 \leq \theta \leq 74.8^\circ$ ). Two reference reflections ([220],  $\bar{1}07$ ) were measured hourly and showed no decrease during the 84 h collecting time. Unit-cell parameters were refined by a least-squares fitting procedure using 23 reflections with  $39.91 \leq \theta \leq 41.70$ . Corrections for Lorentz and polarization effects were applied. Absorption correction was performed with the PLATON program [21], following the method of North et al. [22] using  $\psi$ -scans of five reflections, with coefficients in the range  $0.498$ – $0.988$ . The structure was solved by the PATTY option of the DIRDIF99 program system [23]. The hydrogen atoms were calculated. Full-matrix least-squares refinement on  $F$ , anisotropic for the non-hydrogen atoms and isotropic for the hydrogen atoms, restraining the latter in such a way that the distance to their carrier remained constant at approximately  $1.0$  Å and keeping their atomic displacement parameters fixed at  $U = 0.10$  Å $^2$ , converged to  $R = 0.080$ ,  $R_w = 0.089$ ,  $(\Delta/\sigma)_{\text{max}} = 0.07$ ,  $S = 1.11$ . A weighting scheme  $w = [13 + 0.01 \cdot (\sigma(F_{\text{obs}}))^2 + 0.01 / (\sigma(F_{\text{obs}}))]^{-1}$  was used. The secondary isotropic extinction coefficient [24] refined to  $G = 240$  (64). A final difference Fourier map revealed a residual electron density between  $-1.2$  and  $2.1$  e Å $^{-3}$  in the vicinity of the Pd. Scattering factors were taken from Cromer and Mann [25] and International Tables for X-ray Crystal-

lography [26]. The anomalous scattering of Pd and S was taken into account [27]. All calculations were performed with XTAL3.7 [28], unless stated otherwise.

$[\text{C}_{23}\text{H}_{27}\text{OS}_2\text{Pd}]^+\text{SO}_3\text{CF}_3^-$ ,  $M_r$  627.1, monoclinic,  $P2_1/n$ ,  $a = 8.2790(5)$ ,  $b = 12.2683(9)$ ,  $c = 25.136(8)$  Å,  $\beta = 92.71(2)^\circ$ ,  $V = 2550.2(8)$  Å $^3$ ,  $Z = 4$ ,  $D_x = 1.633$  g cm $^{-3}$ ,  $\lambda(\text{Cu K}\alpha) = 1.5418$  Å,  $\mu(\text{Cu K}\alpha) = 86.12$  cm $^{-1}$ ,  $F(000) = 1272$ , r.t., final  $R = 0.080$  for 4225 observed reflections.

### 3. Results

To study the electronic effect of the donor atom of the ligand, the ligands **a–f** [19] were used to synthesize the corresponding (ligand)Pd(1,1-(CH $_3$ ) $_2$ -C $_3$ H $_3$ )OTf complexes [17] **1a–f** by coupling to  $[(1,1-(\text{CH}_3)_2\text{-C}_3\text{H}_3)\text{PdCl}]_2$  [20] followed by the abstraction of the chloride atom using AgOTf.

#### 3.1. Structure of the complexes (NMR, crystal structures)

As evidenced by the characteristic resonances in  $^1\text{H}$  NMR [12,17], the allyl group is bonded in the  $\pi$ -fashion in all cases. The complexes of the ligands bearing two different donor atoms (**1b** and **1c**) were formed in two isomeric structures. In principle, complexes **1b** and **1c** can exist in four different isomeric structures. The methyl groups of the allyl can be oriented *trans* to P or *trans* to As–N and for both these structures, the allyl can be oriented up or down with respect to the xanthene backbone [12,17]. The isomeric structures can be distinguished by the chemical shift and by comparison of the values of  $J(\text{P–H})$  in different complexes. Unfortunately, the NMR signals of complexes **1b** and **1c** are too broad to allow a definitive assignment based on  $J(\text{P–H})$ . It is known [12] that similar complexes of PN-ligands, are also formed in the two isomers that were identified as the ‘up’ and ‘down’ isomers of the complex in which the substituent on the allyl was oriented *trans* to the phosphorus. We therefore conclude that the different isomers of complexes **1b** and **1c** are also the *trans*-P ‘up’ and ‘down’ isomers (Fig. 6).

We were able to obtain crystals of compound **1f**, suitable for structure determination by X-ray crystallography (Fig. 7). A comparison between the crystal structure of **1f** with those of the bidentate phosphorus analogs mentioned earlier is presented in Table 1.

The distance of the triflate counterion to palladium in complex **1f** is large ( $d(\text{Pd–S}) = 7.152$  Å) and the palladium complex can thus be regarded as a cationic fragment. The structure of **1f** resembles the previously reported crystal structures of analogous complexes bearing bidentate phosphine ligands [2,17,32,33], such as dppe, dppf, DPEphos and Xantphos (Table 1, Fig.

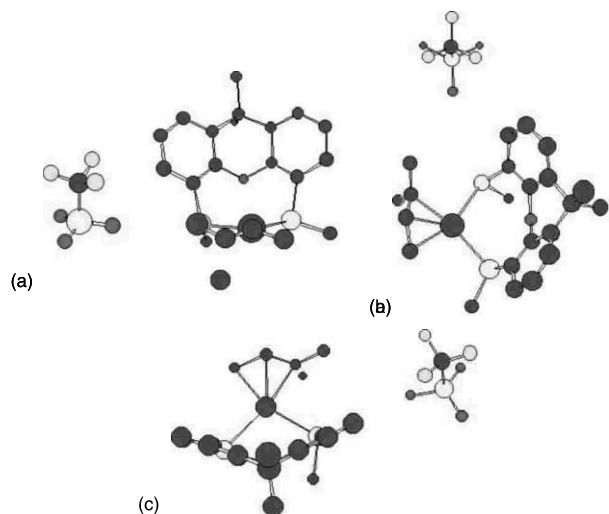


Fig. 7. Three views of the crystal structure of **1f** (hydrogen atoms omitted for clarity): (a) showing the slight rotation of the allyl group; (b) showing the orientation of the Me-substituents on the sulfur atoms; and (c) showing the folding of the xanthene backbone.

3). A more detailed analysis, however, reveals some remarkable features. In the complexes of the PP ligands, the allyl moiety is not bonded symmetrically to the palladium. Compared with the  $C_3H_5$  complex, the C1–C2 bond is elongated and the C2–C3 bond is shortened. At the same time, the Pd–C1 bond is shortened and the Pd–C2 and Pd–C3 bonds are elongated. It was found that for these diphosphine ligands, two phenyl rings are located in the Pd–allyl plane. Therefore, a wide P–Pd–P bite angle results in a large cone angle and, via increased steric interaction of the ligand with the allyl moiety, induces a distorted symmetry of the Pd–allyl bond.

For the disulfide ligand **f**, the observed bite angle of  $103.35(9)^\circ$  is smaller than that found for the analogous diphosphine ligand **a**. The xanthene backbone is not flat, but slightly folded (Fig. 7). The folding of the xanthene backbone in the disulfide ligand **f** is larger than that found for the diphosphine xantphos **a** ( $35.5$  vs.  $27.4^\circ$ ).

In contrast to the phenyl rings of the diphosphine ligand **a**, the methyl substituent on each of the sulfur atoms do not point in the direction of the allyl moiety and the steric interaction of the ligand with the allyl is minimal. The observed Pd–C<sub>allyl</sub> distances are slightly shorter than those found for the diphosphine ligands. In contrast to the complexes with the bidentate phosphine ligands, however, the Pd–C1 and Pd–C3 distances are similar. The C1–C2 distance ( $1.413 \text{ \AA}$ ) is similar to the C1–C2 distance ( $1.42 \text{ \AA}$ ) found for the diphosphine ligands, but the C2–C3 bond ( $1.314 \text{ \AA}$ ) is much shorter. Further, in contrast to the diphosphine-modified complexes, the allyl moiety is rotated around the Pd–allyl axis. The C2 atom is located  $0.17 \text{ \AA}$  above the S–Pd–S plane and the C1 atom is  $0.17 \text{ \AA}$  below the S–Pd–S plane, while C3 is located only  $0.09 \text{ \AA}$  below the S–Pd–S plane. Such a rotated structure has been observed before using a 1,3-diphenyl-allyl moiety and a P–S ligand [29], or a P–N ligand [30].

### 3.2. Stoichiometric alkylation

To study the effect of the donor atom of the ligand on the regioselectivity of the stoichiometric allylic alkylation, complexes **1a–f** were treated with sodium diethyl 2-methylmalonate. The results presented in Table 2 show that the nature of the ligand donor atoms has a

Table 1  
Comparison of selected structural data of crystal structures of allyl complexes of dppe, dppf, DPEphos, xantphos and SS-xanthene (distances in  $\text{\AA}$ ; angles in  $^\circ$ )

Ligand	$C_{31}H_{33}P_2Pd^+CF_3SO_3^-$ dppe <sup>a</sup>	$C_{39}H_{37}FeP_2Pd^+BF_4^-$ dppf <sup>a</sup>	$C_{41}H_{37}OP_2Pd^+BF_4^-$ DPEphos <sup>a</sup>	$C_{42}H_{37}OP_2Pd^+BF_4^-$ Xantphos <sup>a</sup>	$C_{22}H_{30}OS_2Pd^+CF_3SO_3^-$ SS-xanthene ( <b>1f</b> ) <sup>b</sup>
Allyl	$C_3H_3(CH_3)_2$	$C_3H_3(CH_3)_2$	$C_3H_3(CH_3)_2$	$C_3H_5$	$C_3H_3(CH_3)_2$
C1C2	1.42(1)	1.42(2)	1.39(1)	1.34(2)	1.413(10)
C2C3	1.41(1)	1.41(2)	1.28(1)	1.34(2)	1.314(17)
C3C <sub>syn</sub>	1.50(1)	1.44(2)	1.41(2)		
C3C <sub>anti</sub>	1.51(1)	1.58(2)	1.59(2)		
PdC1	2.185(9)	2.192(15)	1.48(1)	2.17(1)	1.428(18)
PdC2	2.174(7)	2.152(16)	1.48(1)	2.16(1)	1.628(18)
PdC3	2.253(7)	2.291(18)	2.21(1)	2.17(1)	2.144(8)
PdL <sub>trans</sub>	2.296(2)	2.313(6)	2.37(1)	2.372(2)	2.123(10)
PdL <sub>cis</sub>	2.293(2)	2.33(9)	2.336(2)	2.372(2)	2.192(10)
$\angle$ (LPdL)	85.77(6)	101.1646	2.379(2)	108.11(7)	2.424(3)
			103.96(3)		2.411(3)
					103.35(9)

<sup>a</sup> Obtained from Ref. [17].

<sup>b</sup> This study.

Table 2

Comparison of the regioselectivity of the stoichiometric alkylation of complexes bearing PP-ligands and of complexes **1a–f**

Ligand	Bite angle	% Branched (A)	% Linear (B)
dppe <sup>a</sup>	85.77(6) <sup>b</sup>	8	92
dppf <sup>a</sup>	101.2(3) <sup>b</sup>	13	87
DPEphos <sup>a</sup>	103.96(3) <sup>b</sup>	41	59
PP-xanthene ( <b>1a</b> ) <sup>a</sup>	108.11(7) <sup>b</sup>	61	39
P–As–xanthene ( <b>1b</b> )	105.4 <sup>c</sup>	38	62
P–N–xanthene ( <b>1c</b> )	106.0 <sup>c</sup>	26	74
As–As–xanthene ( <b>1d</b> )	107.6 <sup>c</sup>	13	87
N–N–xanthene ( <b>1e</b> )	<sup>d</sup>	1	99
S–S–xanthene ( <b>1f</b> )	103.35(9) <sup>b</sup>	5	95

<sup>a</sup> Bite angle determined from crystal structure.

<sup>b</sup> Bite angle determined by semi-empirical PM3(tm) calculations.

<sup>c</sup> Data taken from Ref. [17].

<sup>d</sup> No global minimum could be found using PM3(tm).

pronounced effect on the regioselectivity of the reaction. The branched/linear product distribution ranges from 1/99 (A/B) for complex **1e** to 60/40 (A/B) for complex **1a**. Thus, the bidentate nitrogen ligand **e** is much more selective in forming the linear product **B** than any of the bidentate phosphorus ligands used earlier.

## 4. Discussion

### 4.1. Mechanism, hypothesis

Much has been reported concerning the mechanism of the palladium catalyzed allylic alkylation [1–17]. Both experimental and theoretical studies support a mechanism via a late transition state, i.e. in the transition state the allyl moiety resembles the olefin product [1–3]. In contrast, some results seemed to support an *early* transition state model in which the regioselectivity is determined by electronic factors in the  $\pi$ -allyl complex [11–14,16,17]. In summary, the relative importance of steric and electronic factors depends on the bite angle of the ligand, on the nature of the substituents (e.g. phenyl or methyl) and on the orientation of the substituents (*syn* or *anti*) [12,13,16,17]. The results presented in this paper can be explained in terms of these effects. In addition to the factors mentioned above, the nature of the donor atoms (donor/acceptor

properties) is also important for the transition state of the reaction.

### 4.2. Effect of the nature of the donor atoms on the structure

It has been proposed that the regioselectivity of the reaction depends on the distortion of the symmetry of the Pd–allyl bond, which in turn depends on both steric and electronic factors [11,12,17]. In the present series of ligands, the steric bulk (cone angle) will be approximately the same for all ligands (except for the disulfide ligand). The various donor atoms used in this paper differ significantly in donor and acceptor properties. A decrease in  $\sigma$ -donation from the ligand to the metal will result in a decrease of electron density on the palladium and consequently will lead to an increase of the bonding interaction from the allyl to palladium. Analogously, a decrease in the  $\pi$ -back donation from the metal to the ligand will result in an increase of electron density in the  $\pi$ -system of the palladium atom and the  $\pi$ -back donation from the palladium to the allyl moiety will be enhanced. The ligand causes a change in the donating–bonding interaction of the allyl to the metal. This does not affect the allyl-LUMO, but the effect of the ligand on the  $\pi$ -back donation of the palladium to the ligand *does* influence the energy level of the allyl-LUMO. A weak  $\pi$ -acceptor ligand causes more  $\pi$ -back donation to the allyl, which results in a higher energy level of the anti-bonding combination of the Pd–allyl bond, and consequently a less electrophilic allyl moiety [31]. Further, an increase in the  $\pi$ -back donation to the allyl will result in an increase in the symmetry of the Pd–allyl bond. This is reflected in the crystal structure of **1f**, in which the Pd–allyl bond is shorter and much less distorted than in the corresponding diphosphine complexes.

In addition, the absence of steric interaction between the ligand and the allyl group in **1f** results only in a relatively small distortion of the Pd–allyl bond. The allyl itself resembles the structure of an internal olefin. The Pd–C3 distance, however, is only slightly larger than the Pd–C1 distance, whereas in the structures of the complexes bearing bidentate phosphine ligands, the Pd–C1 distance is much shorter than the Pd–C3 distance. The C2–C3 bond in **1f** is much shorter than the C1–C2 bond and is mainly olefinic in nature.

In the complexes bearing the ligands **b–e** with less strong  $\pi$ -accepting donor atoms, the allyl group will be deformed. Because the steric interaction of the allyl with the phenyl rings of these ligands will be much larger than with the methyl groups of ligand **f**, the  $\eta^1$ – $\eta^2$  type distortion of the Pd–allyl bond as found for the diphosphine ligands can be expected for steric reasons.

### 4.3. Effect of the nature of the donor atom on the regioselectivity

In the case of the diphosphine ligand **a**, attack on C3 is favored for electronic reasons [17]. On nucleophilic attack, the two methyl substituents on the allyl rotate out of the P–Pd–P plane and the steric interaction with the phenyl rings of the ligand will be minimized during the rotation of the allyl group [2]. On the other hand, allyl rotation after nucleophilic attack on C1 will leave the methyl substituents in the P–Pd–P plane, thereby maximizing the steric interactions with the phenyl rings. In the case of a late transition state, the relative thermodynamic stability of the products may become an important factor and the formation of the internal olefin **B** may be favored.

The selectivity for the formation of the branched product (terminal olefin **A**) decreases with decreasing  $\pi$ -accepting properties of the ligand donor atoms. Thus, going from P–P (**a**) to N–N (**e**), the allyl moiety compensates for the weaker  $\pi$ -accepting properties of the ligand and becomes less electrophilic. In other words, the allyl-LUMO will be higher in energy for the complex bearing the bidentate nitrogen ligand. The energy gain on nucleophilic attack will be less than those for the diphosphine modified complex and it is therefore more likely that the C–C bond formation is reversible for the diamine complex. Thus, the formation of the branched product **A** is favored for the diphosphine ligand as a result of the relative electrophilicity of C1 and C3, whereas product **B** is favored for the bidentate nitrogen ligand as a result of its relative thermodynamic stability.

For ligands **a–f**, the regioselectivity of the mixed ligands is in between the results of the corresponding symmetric ligands. This statement does not apply to other mixed ligands, since many examples of mixed P–N ligands that favor the formation of the branched product with up to 99% regioselectivity are known [5–8].

In complexes **1b** and **1c**, C3 will be more electrophilic than C1, which is reflected in the observed regioselectivity. For the P–As complex (**1b**), the strong  $\pi$ -acceptor properties of the phosphorus results in an increase of the selectivity for product **A** relative to the As–As complex (**1d**). Analogously, the weaker  $\pi$ -acceptor properties of the arsine lead to a decrease of the selectivity for product **A** compared with the diphosphine complex (**1a**).

## 5. Conclusions

In the allylic alkylation catalyzed by Pd complexes with bidentate ligands based on a xanthene backbone, the donor atoms have a pronounced influence on the

regioselectivity of the reaction. The formation of the branched product **A** is relatively favored for the ligands bearing the stronger  $\pi$ -acceptor, whereas the ligands bearing the weaker  $\pi$ -acceptors favor the linear product **B**. The results are explained in terms of the relative electrophilicity of the non-substituted C1 atom (leading to **B**) compared with that of the substituted C3 atom (leading to **A**).

We propose that the overall regioselectivity of the reaction is determined by three factors:

1. The relative electrophilicity of C1 and C3.
2. The overall electrophilicity of the allyl moiety.
3. The thermodynamic stabilities of the products.

## Acknowledgements

This research was carried out with financial support from DSM Research B.V. and with a subsidy from the Ministerie van Onderwijs, Cultuur en Wetenschappen as part of the E.E.T. program for clean chemistry.

## References

- [1] (a) B.M. Trost, D.V. van Vranken, *Chem. Rev.* 96 (1996) 395; (b) A. Pfaltz, *Acc. Chem. Res.* 26 (1993) 339.
- [2] (a) P. Dierkes, S. Ramdeehul, L. Barloy, A. de Cian, J. Fischer, P.C.J. Kamer, P.W.N.M. van Leeuwen, J.A. Osborn, *Angew. Chem., Int. Ed. Engl.* 37 (1998) (1998) 3116; (b) S. Ramdeehul, P. Dierkes, R. Aguado, P.C.J. Kamer, P.W.N.M. van Leeuwen, J.A. Osborn, *Angew. Chem., Int. Ed. Engl.* 37 (1998) 3118.
- [3] P.E. Blochl, A. Togni, *Organometallics* 15 (1996) 4125.
- [4] (a) K. Vrieze, P.W.N.M. van Leeuwen, *Prog. Inorg. Chem.* 14 (1971) 1; (b) K. Vrieze, H.C. Volger, P.W.N.M. van Leeuwen, *Inorg. Chim. Acta, Rev.* 3 (1969) 109.
- [5] R. Pretot, A. Pfaltz, *Angew. Chem., Int. Ed. Engl.* 37 (1998) 323.
- [6] S. Vyskocil, M. Smrcina, V. Hanus, M. Polasek, P. Kocovsky, *J. Org. Chem.* 63 (1998) 7738.
- [7] R. Pretot, G.C. Lloyd-Jones, A. Pfaltz, *Pure Appl. Chem.* 70 (1998) 1035.
- [8] H. Steinhausen, M. Reggelin, G. Helmchen, *Angew. Chem., Int. Ed. Engl.* 36 (1997) 2108.
- [9] G.E. Oosterom, R.J. van Haaren, J.N.H. Reek, P.C.J. Kamer, P.W.N.M. van Leeuwen, *Chem. Commun.* (1999) 1119.
- [10] M. Kranenburg, P.C.J. Kamer, P.W.N.M. van Leeuwen, *Eur. J. Inorg. Chem.* (1998) 25.
- [11] J.D. Oslob, B. Åkermark, P. Helquist, P.-O. Norrby, *Organometallics* 16 (1997) 3015 (and references therein).
- [12] R.J. van Haaren, C.J.M. Drujven, G.P.F. van Strijdonck, H. Oevering, J.N.H. Reek, P.C.J. Kamer, P.W.N.M. van Leeuwen, *J. Chem. Soc., Dalton Trans.* (2000) 1549.
- [13] R.J. van Haaren, H. Oevering, B.B. Coussens, G.P.F. van Strijdonck, J.N.H. Reek, P.C.J. Kamer, P.W.N.M. van Leeuwen, *Eur. J. Inorg. Chem.* (1999) 1237.
- [14] H. Hagelin, B. Åkermark, P.-O. Norrby, *Chem. Eur. J.* 5 (1999) 902.
- [15] V. Blanchadell, M. Moreno-Manas, F. Pajuelo, R. Pleixats, *Organometallics* 18 (1999) 4934.



- [16] R.J. van Haaren, G.P.F. van Strijdonck, H. Oevering, J.N.H. Reek, P.C.J. Kamer, P.W.N.M. van Leeuwen, *Eur. J. Inorg. Chem.* (2001) 837.
- [17] R.J. van Haaren, K. Goubitz, J. Fraanje, G.P.F. van Strijdonck, H. Oevering, B.B. Coussens, J.N.H. Reek, P.C.J. Kamer, P.W.N.M. van Leeuwen, *Inorg. Chem.* 40 (2001) 3363.
- [18] (a) P. Wehman, R.E. Rulke, V.E. Kaasjager, P.C.J. Kamer, H. Kooijman, A.L. Spek, C.J. Elsevier, K. Vrieze, P.W.N.M. van Leeuwen, *J. Chem. Soc., Chem. Commun.* (1995) 331;  
(b) R.E. Rulke, V.E. Kaasjager, P. Wehman, C.J. Elsevier, P.W.N.M. van Leeuwen, K. Vrieze, J. Fraanje, K. Goubitz, A.L. Spek, *Organometallics* (1996) 3022;  
(c) H.A. Ankersmit, B.H. Loken, H. Kooijman, A.L. Spek, K. Vrieze, G. van Koten, *Inorg. Chim. Acta* (1996) 141.
- [19] (a) L.A. van der Veen, P.K. Keeven, P.C.J. Kamer, P.W.N.M. van Leeuwen, *Chem. Commun.* (2000) 333;  
(b) L.A. van der Veen, P.K. Keeven, P.C.J. Kamer, P.W.N.M. van Leeuwen, *J. Chem. Soc., Dalton Trans.* (2000) 2105.
- [20] W.D. Dent, R. Long, A.J. Wilkinson, *J. Chem. Soc.* (1964) 1585.
- [21] A.L. Spek, *Acta Crystallogr., Sect. A* 46 (1990) 34.
- [22] A.C.T. North, D.C. Phillips, F. Scott Mathews, *Acta Crystallogr., Sect. A* 26 (1969) 351.
- [23] P.T. Beurskens, G. Beurskens, R. Gelder, S. Garcia-Granda, R.O. Gould, R. Israel, J.M.M. Smits, The DIRDIF99 Program System, Crystallography Laboratory, University of Nijmegen, The Netherlands, 1999.
- [24] (a) A.C. Larson, in: F.R. Ahmed, S.R. Hall, C.P. Huber (Eds.), *Crystallographic Computing*, 2nd ed., Munksgaard, Copenhagen, 1969, p. 291;  
(b) W.H. Zachariasen, *Acta Crystallogr., Sect. A* 23 (1967) 558.
- [25] D.T. Cromer, J.B. Mann, *Acta Crystallogr., Sect. A* 24 (1968) 321.
- [26] *International Tables for X-ray Crystallography*, vol. IV, Kynoch Press, Birmingham, 1974, p. 55.
- [27] D.T. Cromer, D. Liberman, *J. Chem. Phys.* 53 (1970) 1891.
- [28] S.R. Hall, D.J. du Boulay, R. Olthof-Hazekamp (Eds.), *XTAL3.7 System*, University of Western Australia, Lamb, Perth, 2000.
- [29] A. Albinati, P.S. Pregosin, K. Wick, *Organometallics* 15 (1996) 2419.
- [30] (a) K. Selvakumar, M. Valentini, M. Worle, P.S. Pregosin, A. Albinati, *Organometallics* 18 (1999) 1207;  
(b) K. Selvakumar, M. Valentini, P.S. Pregosin, *Organometallics* 18 (1999) 4591.
- [31] K.J. Szabo, *J. Am. Chem. Soc.* (1996) 7818.
- [32] A. Knierzinger, P. Schonholzer, *Helv. Chim. Acta* 75 (1992) 1211.
- [33] P.S. Pregosin, H. Ruegger, R. Salzmann, A. Albinati, F. Lianza, R.W. Kunz, *Organometallics* 13 (1994) 83.